

NATIONAL INSTITUTE FOR FUSION SCIENCE**Stimulated Electron-Acoustic-Wave
Scattering in a Laser Plasma**

Lj. Nikolić, M.M. Škorić, S. Ishiguro and T. Sato

(Received - July -26, 2002)

NIFS-738

Aug. 2002

This report was prepared as a preprint of work performed as a collaboration research of the National Institute for Fusion Science (NIFS) of Japan. The views presented here are solely those of the authors. This document is intended for information only and for future publication in a journal after some rearrangements of its contents.

Inquiries about copyright and reproduction should be addressed to the Research Information Center, National Institute for Fusion Science, Oroshi-cho, Toki-shi, Gifu-ken 509-5292 Japan.

RESEARCH REPORT
NIFS Series

Stimulated Electron-Acoustic-Wave Scattering in a Laser Plasma

Lj. Nikolić¹, M. M. Škorić², S. Ishiguro³ and T. Sato⁴

¹*The Graduate University for Advanced Studies*

²*Vinča Institute of Nuclear Sciences, Yugoslavia*

³*National Institute for Fusion Science*

⁴*Earth-Simulator Center*

Abstract

Intense laser-plasma interaction can be a source of various electronic instabilities. Recently, stimulated backscattering from a trapped electron-acoustic wave (SEAS) (D. S. Montgomery *et al.*, Phys. Rev. Lett. **87**, 155001 (2001)) was proposed to reinterpret spectra previously attributed to stimulated Raman scattering (SRS) from unrealistically low densities. By particle simulations in a uniform plasma layer, which is overdense for ordinary SRS, strong reflection by SEAS at the electron plasma frequency is found. Transient SEAS reflectivity pulsations are followed by strong relativistic heating of electrons. Physical conditions are explained by three-wave parametric coupling between laser light, standing backscattered wave and slow electron-acoustic wave. Regions in which SEAS reflection can dominate over SRS are singled out.

KEYWORDS: laser-plasma interaction, particle simulation, Raman scattering, acoustic scattering

The propagation of a laser light through an under-dense plasma is an active research topic. Much works have been devoted to stimulated Raman and Brillouin scattering instabilities, concerning their ability to produce energetic particles which can preheat the core of a fusion pellet. The stimulated scattering from an electron plasma wave (EPW) (Raman scattering - SRS) or ion acoustic wave (IAW) (Brillouin scattering - SBS) can be large to reflect a significant part of the laser light and decrease the coupling efficiency at the target. As was shown by experiments and computer simulations there can be a rich interplay between these two instabilities [1-3]. Although understanding of basic principles of laser parametric coupling to the EPW and IAW is quite satisfactory, the quantitative predictions are often in large disagreement with observations from real experiments. There is a recent upsurge of interest to explain unexpectedly high SRS reflectivity obtained in experiments emulating conditions of National Ignition Facility targets [4,5].

More recently, D. S. Montgomery *et al.* reported observation of a novel stimulated electron-acoustic wave scattering (SEAS) to explain "single hot spot" experiments performed at Trident laser facility [6]. Namely, in the linear theory, the so-called electron-acoustic wave (EAW) exists, i.e. a strongly damped

linearized Vlasov-Maxwell (VM) mode whose phase velocity is between an EPW and an IAW; often neglected in studies of wave-plasma instabilities. However, analytical studies of non-linear one-dimensional VM solutions have found that strong electron trapping can occur even for small amplitude electrostatic wave, resulting in undamped non-linear travelling waves (BGK-like) [7,8] or, with an inclusion of small dissipation, in weakly damped travelling solutions [9]. The main difficulty in resolving SEAS from the standard SRS in laser-plasma experiments is that the backscattered light spectrum can cover the nearly continuous broad range of frequencies due to a simultaneous growth of instabilities at different spatial locations in a non-uniform plasma, complex wave-plasma dynamics due to the system length, etc. The first observation of backward SEAS and reinterpretation of earlier experimental results from low plasma densities [6], has encouraged further investigation of domains and conditions for SEAS. However, under reported conditions the energy in the SEAS mode still remained well below (3000 times) the observed backward SRS level.

In this paper, excitation of SEAS and its interconnection with SRS instability is investigated by particle simulation of a propagation of a linearly polarized laser through a plasma layer placed in vac-

uum. An electromagnetic relativistic 1d3v PIC code was used. The number of grids was 25 per $1c/\omega_0$ (ω_0 is the laser frequency), with minimum 50 particles/grid. The length of a simulation system was $220c/\omega_0$ and ions were kept immobile as a neutralizing background. The electrons which enter vacuum build a potential barrier that prevents other electrons of leaving the plasma. However, due to strong heating some energetic electrons can reach boundaries of the system. For these electrons, as well as for electromagnetic waves additional damping regions were used. In number of simulations, besides stimulated Raman backscattering, we have observed an intense reflection recognized as SEAS instability, with its main contribution in regions with over-critical density for ordinary SRS. Strong SEAS reflection, which can several times exceed SRS reflectivity, is followed by large heating of a plasma. To our knowledge, we are first to report such a plasma behavior.

From our simulation data SEAS is identified as a resonant three-wave parametric interaction [10] involving the laser pump (ω_0, k_0), the backscattered lightwave (ω_s, k_s) and the trapped electron-acoustic wave (EAW) (ω_a, k_a). In the linear instability stage, resonant conditions $\omega_0 = \omega_s + \omega_a$ and $k_0 = -k_s + k_a$ are well satisfied, while electromagnetic waves (pump and Stokes wave) satisfy standard dispersion equation $\omega_{0,s}^2 = \omega_p^2 + c^2 k_{0,s}^2$. The backscattered wave is always found to be driven near critical, i.e. $\omega_s \approx \omega_p$ which implies $k_s \approx 0$ and $V_s \approx 0$ ($\omega_p = (ne^2/(\epsilon_0 m \gamma))^{1/2}$ is the plasma frequency, γ is the relativistic factor, and $V_s = c^2 k_s / \omega_s$ is the light group velocity). Therefore, the Stokes sideband is a slowly propagating, almost standing electromagnetic wave. The above decay scheme is observed for a wide range of laser intensities, plasma densities and temperatures. It is known that high temperatures can significantly alter the growth rates and sometimes suppress parametric instabilities [11]. However, according to [9], efficient excitation of trapped EAW ($\omega_a < \omega_p$), is to be expected in the range $v_{ph}/v_t = 1 - 2$ (v_{ph} and $v_t = (T/m)^{1/2}$ are the phase and electron thermal velocities). Thus, for SEAS excitation at the threshold, high thermal velocity which closely match the EAW phase velocity is important. To illustrate an onset and growth of SEAS instability, spectra of electromagnetic-light (EM) waves and electrostatic (ES) waves are plotted in Figs. 1-2.

Fig. 1 shows discrete spectra in an early phase of SEAS instability. The density and the plasma length are $n = 0.6n_{cr}$ ($n_{cr} = n(\omega_0/\omega_p)^{1/2}$) and $L = 40c/\omega_0$, respectively, the longitudinal thermal velocity is $v_t/c = 0.28$ and the laser strength is $\beta = (eE_0)/(mc\omega_0) = 0.3$ (E_0 is the amplitude of the electric field). The backscattered EM wave grows

at the electron plasma frequency $\omega_p \approx 0.72\omega_0$ (the laser pump line at $\omega/\omega_0 = 1$ is not shown), while corresponding EAW is at $\omega_0 - \omega_p \approx 0.28\omega_0$. Note that apart from ES noise around a natural plasma mode ($\omega_p \approx 0.72\omega_0$), ponderomotively driven non-resonant modes are also present (not shown in Fig. 1) at 2-nd, $\omega = 2\omega_0$ and $k = 2k_0$ ($v_{ph}/c \approx 1.44$), as well as at zero-harmonic [12]. From obtained data, it follows that the phase velocity of the EAW is $v_{ph}/c = (\omega_0 - \omega_p)/k_0 \approx 0.41$.

In Fig. 2 nonlinearly broadened EM and ES spectra of fully developed SEAS are shown for a plasma with $n = 0.4n_{cr}$, $L = 40c/\omega_0$, $v_t/c = 0.20$ and laser strength $\beta = 0.3$. The instability growth results in the plasma frequency decrease and strong electron heating which tends to suppress the further growth. Above is reconfirmed in the post -SEAS stage, after the instability was halted (vide infra). Once EAW has died off, dominant ES response is weak EPW, which peaks at perturbed $\omega_p \approx 0.54\omega_0$ (the decrease of 0.06 from the initial state), while the decreased Stokes sideband appears at $\omega_s \approx 0.58\omega_0$. Moreover, a blue-shifted, modulated and incoherently broadened EM spectrum (Fig. 2) seems consistent with the three-wave backscatter complexity induced by the nonlinear phase, as recently predicted by some of these authors [5,15].

We propose a SEAS model as a resonant parametric coupling of three waves $a_i(x, t) \exp[i(k_i x - \omega_i t)]$, in a weakly varying envelope approximation [13-15],

$$\frac{\partial a_0}{\partial t} + V_0 \frac{\partial a_0}{\partial x} = -M_0 a_s a_a, \quad (1)$$

$$\frac{\partial a_s}{\partial t} - V_s \frac{\partial a_s}{\partial x} = M_s a_0^* a_a, \quad (2)$$

$$\frac{\partial a_a}{\partial t} + V_a \frac{\partial a_a}{\partial x} + \Gamma_a a_a = M_a a_0^* a_s, \quad (3)$$

where $V_i > 0$ are the group velocities, Γ_a is damping rate for EAW ($\Gamma_0 = \Gamma_s = 0$ for light waves is used), $M_i > 0$ are the coupling coefficients and a_i are the wave amplitudes, where $i = 0, s, a$, stand for the pump, backscattered wave and EAW, respectively. Since considered model is a short plasma, in order to get high reflectivity, instability needs to be absolute. With standard boundary conditions $a_0(0, t) = E_0$, $a_s(L, t) = a_a(0, t) = 0$, the backscattering becomes an absolute instability if

$$L/L_0 > \pi/2, \quad (4)$$

[13,14], where $L_0 = (V_s V_a)^{1/2} / \gamma_0$ is the interaction length and $\gamma_0 = E_0 (M_s M_a)^{1/2}$ is the uniform growth rate. Since observed $V_s \approx 0$ for the backscatter, the condition (4) is readily satisfied ($L_0 \approx 0$). Explicit

form of (1) and (2) is easy to get (light waves), however for EAW (3) no linear dispersion relation in analytical form exists [6-9]. Since damping rate $\Gamma_a \neq 0$, the EAW is characterized by the longitudinal absorption length $L_a = V_a/\Gamma_a$, SEAS-backscatter instability becomes absolute under an extra condition [14],

$$L_0/L_a < 2. \quad (5)$$

In a linear theory EAW is a highly damped mode, so the absorption length L_a is taking small values. However, as concluded earlier, the key factor for an onset and growth of SAES is nearly critical "standing" backward Stokes wave ($L_0 \approx 0$), so that $V_s \approx 0$ satisfies (5) and also minimizes the threshold E_0 for SEAS instability [14], $\gamma_0 > 0.5\Gamma_a(V_s/V_a)^{1/2}$.

The temperature effect can be clearly seen near the threshold intensity for SEAS ($\beta \sim 0.3$). Since the longitudinal thermal velocity of electrons can easily increase due to e.g. the Raman instability, the temperature in transverse direction was set to 500eV, with a longitudinal temperature taken as a control parameter. However, we note, that the SEAS instability was readily observed for isotropic distribution, as well. Just above the threshold, high electron temperature may be essential for an instability growth. This is illustrated by Fig. 3 in which reflectivity ($R = \langle S_r \rangle / \langle S_0 \rangle$, S_r and S_i are Poynting vectors for reflected and incident wave, respectively, and $\langle \rangle$ denotes time averaged values) are shown for $\beta = 0.3$, $n = 0.4n_{cr}$, $L = 40c/\omega_0$ at several temperatures, $v_t/c = 0.19, 0.20, 0.28$ and 0.30 . There is an optimum temperature for perfect matching with an excited EAW which results in a maximum SEAS reflectivity. For $v_t/c = 0.2$ observed reflectivity is very high - nearly 140% of the incident laser light. One calculates $v_{ph}/v_t \approx 2.64, 2.50, 1.84$ and 1.72 for $v_t/c = 0.19, 0.20, 0.28$ and 0.30 , respectively. For temperatures $\leq v_t/c = 0.18$ and $\beta = 0.3$ the instability was not observed during time period of $t\omega_0 = 5000$.

For laser intensities well above the threshold there appears no need for high electron temperatures to excite SEAS. For example, already at $T = 500\text{eV}$, with a strong relativistic pump $\beta = 0.6$, $n = 0.6n_{cr}$ and $L = 40c/\omega_0$ instability develops fast and quickly saturates within $t\omega_0 = 500$. In Fig. 4, time evolution of SEAS reflectivity and the electron distribution function $f(v_x/c)$ for the initial ($t\omega_0 = 0$) and the state after the instability ($t\omega_0 = 1000$) are plotted. This effect, seems related to relativistic interactions, important for e.g. fast ignitor research, and will deserve future attention. First estimates point out at the relativistic-nonlinear frequency shift (NLFS) of the electrostatic wave driven by a laser, as a possible cause [12]. At relativistic intensity, large NLF generates broad ES harmonics which can cover resonant EAW frequency. SEAS resonance is broadened,

while instability can grow rapidly, instead from a low background noise, directly from a finite ES harmonic, seeded by a laser. As seen in Fig. 4, SEAS produces large relativistic heating which deforms an initial Maxwellian into "water-bag" alike distribution and generates highly energetic electrons with main contribution near $v = \pm v_{ph}$ of the EAW.

Finally, we briefly address a question of coexistence and interrelation between SRS and SEAS. The simulated system consists of two connected underdense plasma layers L_1 and L_2 , of the length $L_1 = 20c/\omega_0$ and $L_2 = 80c/\omega_0$ with corresponding densities $n_1 = 0.2n_{cr}$ and $n_2 = 0.6n_{cr}$, respectively. Initial temperature is taken at 500eV. Our choice of densities makes L_1 strongly active for Raman instability, while L_2 (overdense for SRS) is practically in a role of a heat sink. Simulations show common picture, an excitation of strong SRS marked by intermittent reflectivity pulsations (see Fig. 5, $t\omega_0 < 1000$) [5,15]. The instability eventually gets suppressed by strong heating of supra-thermal and bulk electrons. Since hot electrons quickly escape the Raman region (L_1) they enter and heat the sink (L_2). Moreover, a striking feature emerges at late times, with a reflection of a second intense pulse much larger than the original Raman signal (Fig. 5, $t\omega_0 \approx 2700$). This is readily identified as SEAS which originates from the large "sink", once the temperature has grown to resonate with EAW to enable excitation of SEAS. Therefore, SEAS mediated by SRS becomes a dominant process, as an example of a complex interplay possibly relevant to our understanding of future experiments.

In summary, in first particle simulations in a plasma not accessible to SRS, strong isolated SEAS reflection from trapped EAW was observed near the electron plasma frequency. A three-wave parametric model was discussed, in particular, a role of a standing Stokes sideband for excitation of an absolute SEAS instability. While in reported experiments [6] SEAS to SRS signal ratio was smaller than 10^{-3} , we find conditions in which SEAS dominates over standard SRS. Further study of SEAS role, e.g. in relativistic laser-plasmas, deserves future attention.

Acknowledgments

One of us (Lj. N.) acknowledges GUAS scholarship by the Ministry of Education, Science, Sports and Culture of Japan. The authors wish to thank H. Takamaru for his PIC code. This work was supported in parts by Project 1964 of the Ministry of Science and Technology of Republic of Serbia.

References

- [1] W. L. Kruer *et al.*, Phys. Scripta T **75**, 7 (1998).
- [2] D. S. Montgomery *et al.*, Phys. Plasmas **5**, 1973 (1998).
- [3] R. L. Berger *et al.*, Phys. Plasmas **5**, 4337 (1998).
- [4] J. C. Fernández *et al.*, Phys. Plasmas **7**, 3743 (2000).
- [5] H. X. Vu *et al.*, Phys. Rev. Lett. **86**, 4306 (2001).
- [6] D. S. Montgomery *et al.*, Phys. Rev. Lett. **87** (2001); *ibid* Phys. Plasmas **9**, 2311 (2002).
- [7] H. Schamel, Phys. Plasmas **7**, 4831 (2000).
- [8] J. P. Holloway and J. J. Dornig, Phys. Rev. A **44**, 3856 (1991).
- [9] H. A. Rose and D. A. Russell, Phys. Plasmas **8**, 4784 (2001).
- [10] K. Mima and K. Nishikawa, in *Basic Plasma Physics II*, edited by A. A. Galeev and R. N. Sudan, (North-Holland, Amsterdam 1984), p. 451.
- [11] Z.-M. Sheng *et al.*, Phys. Rev. E **61**, 4362 (2000).
- [12] F. W. Sluijter and D. Montgomery, Phys. Fluids **8**, 551 (1965); D. Montgomery and D. A. Tidman, *ibid* **7**, 242 (1964).
- [13] R. W. Harvey and G. Schmidt, Phys. Fluids **18**, 1395 (1975).
- [14] D. W. Forslund *et al.*, Phys. Fluids **18**, 1002 (1975).
- [15] S. Miyamoto *et al.*, J. Phys. Soc. Jpn. **67**, 1281 (1998); M. M. Škorić *et al.*, Phys. Rev. E **53**, 4056 (1996).

Figure captions

- Fig. 1.** Spectrum of electromagnetic (top) and electrostatic (bottom) waves in the plasma layer ($n = 0.6n_{cr}$, $L = 40c/\omega_0$) for time interval $t\omega_0 = 322 - 1379$. The initial electron thermal velocity is $v_t/c = 0.28$.
- Fig. 2.** Spectrum of electromagnetic (top) and electrostatic (bottom) waves in the plasma layer ($n = 0.4n_{cr}$, $L = 40c/\omega_0$) for time interval $t\omega_0 = 1291 - 2348$. The initial electron thermal velocity is $v_t/c = 0.2$.
- Fig. 3.** Reflectivity in time from the plasma layer ($n = 0.4n_{cr}$, $L = 40c/\omega_0$) for different initial electron thermal velocities v_t/c and $\beta = 0.3$.
- Fig. 4.** Reflectivity in time (top) and electron velocity distribution (bottom) in the plasma layer ($n = 0.6n_{cr}$, $L = 40c/\omega_0$, $\beta = 0.6$) for $t\omega_0 = 0$ and $t\omega_0 = 1000$ (after the instability).
- Fig. 5.** Time history of the reflectivity from two connected plasma layers ($n_1 = 0.2n_{cr}$, $L_1 = 20c/\omega_0$, $n_2 = 0.6n_{cr}$, $L_2 = 80c/\omega_0$, $\beta = 0.3$). Initial reflectivity bursts from ordinary SRS in L_1 are followed at late times by a huge SEAS pulse generated in L_2 , which was heated by hot electrons from L_1 .

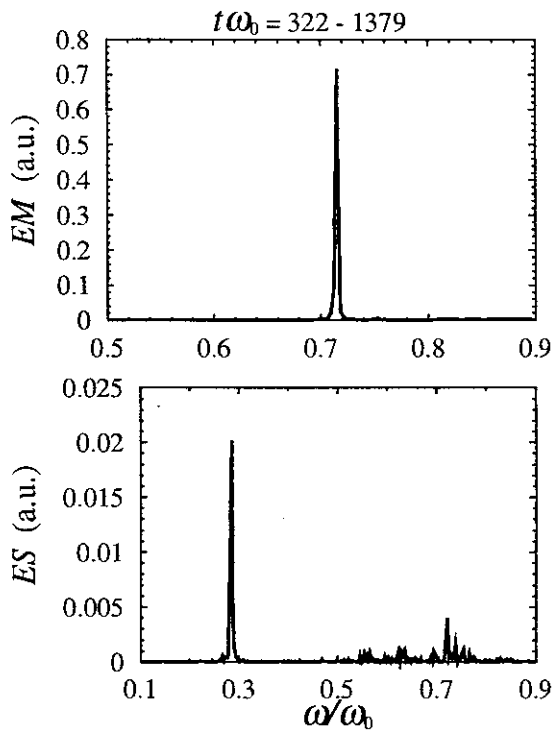


Fig. 1

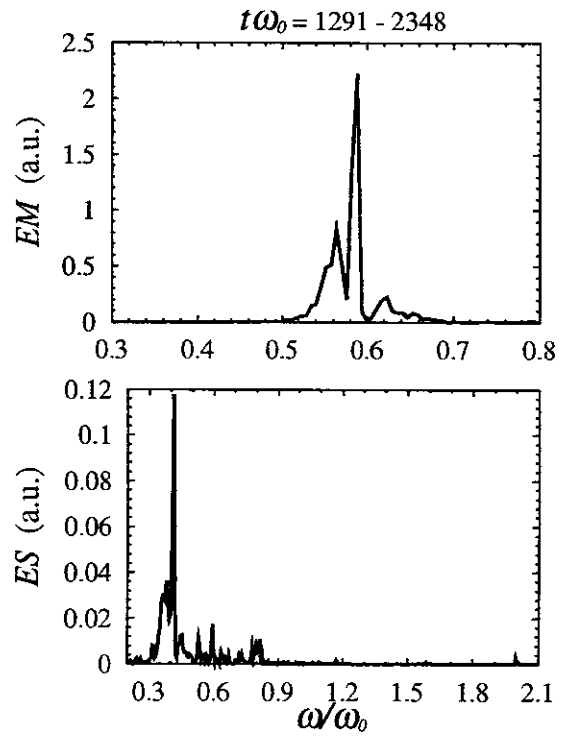


Fig. 2

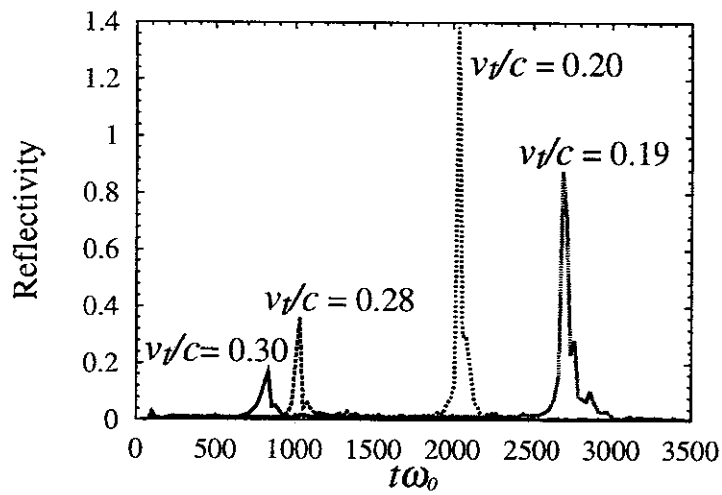


Fig. 3

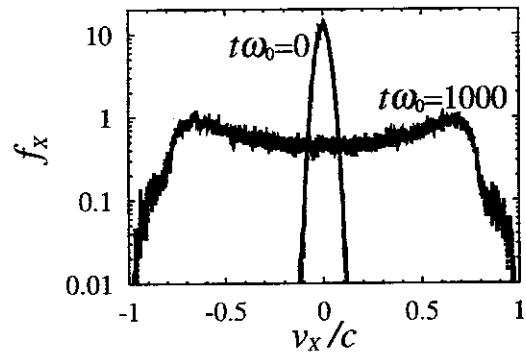
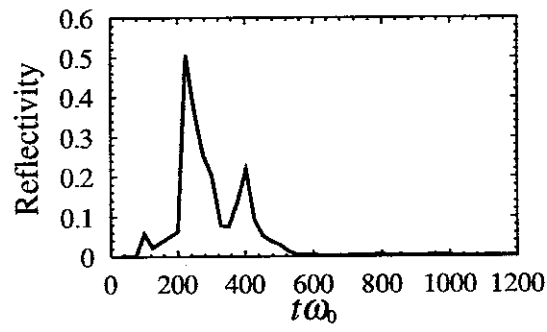


Fig. 4

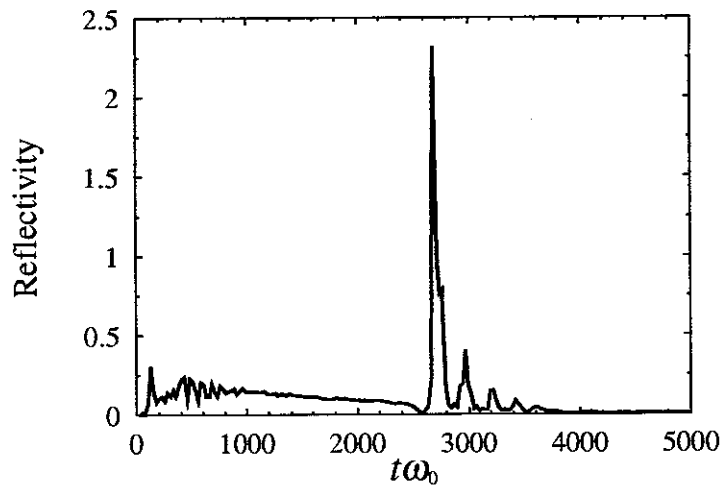


Fig. 5